Univerzita Komenského v Bratislave

Fakulta matematiky, fyziky a informatiky

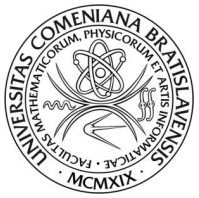

Mgr. Jozef Genzor

Autoreferát dizertačnej práce

Tensor Networks: Phase Transition Phenomena on Hyperbolic and Fractal Geometries

na získanie vedecko-akademickej hodnosti *philosophiae doctor* v odbore doktorandského štúdia: 4.1.2 Všeobecná fyzika a matematická fyzika

BRATISLAVA, 2016

Dizertačná práca bola vypracovaná v dennej forme doktorandského štúdia na školiacom pracovisku: Centrum pre výskum kvantovej informácie, Fyzikálny ústav Slovenskej akadémie vied.

Predkladateľ:	Mgr. Jozef Genzor Centrum pre výskum kvantovej informácie Fyzikálny ústav Slovenská akadémia vied Dúbravská cesta 9 845 11 Bratislava
Školiteľ:	Mgr. Andrej Gendiar, PhD. Centrum pre výskum kvantovej informácie Fyzikálny ústav SAV Bratislava
Oponenti:	

Obhajoba dizertačnej práce sa koná dňa ..... o .....h pred komisiou pre obhajobu dizertačnej práce v odbore doktorandského štúdia vymenovanou predsedom odborovej komisie dňa .....

4.1.2 Všeobecná fyzika a matematická fyzika

na

Predseda odborovej komisie:

prof. RNDr. Peter Prešnajder, DrSc.
Katedra teoretickej fyziky a didaktiky fyziky
Fakulta matematiky, fyziky a informatiky
Univerzita Komenského
Mlynská dolina
842 48 Bratislava

Abstrakt

Jedným z dôležitých problémov fyziky kondenzovaných látok je pochopiť, čo sa odohráva na pozadí mechanizmov kvantových mnohočasticových systémoch. Keďže existuje iba niekoľko úplných analytických riešení pre tietosystémy, v posledných rokoch bolo navrhnutých niekoľko numerických simulačných metód. Spomedzi nich začínajú byť populárne práve tie algoritmy, ktoré sú založené na princípoch tenzorových sietí, a to najmä vďaka ich aplikovateľnosti na simulácie silno korelovaných systémov. Predkladaná práca sa sústreďuje na zovšeobecnenie takýchto algoritmov, ktoré využívajú algoritmus tenzorových sietí a zároveň sú dostatočne robustné na to, aby popísali kritické javy a fázove prechody multispinových Hamiltoniánov v termodynamickej limite. Na to je však nevyhnutné zaoberať sa so systémami s nekonečne veľkým množstvom interagujúcich častíc. Pre tento účel sme si zvolili dva algoritmy, ktoré sú vhodné pre spinové systémy: Corner Transfer Matrix Renormalization Group a Higher-Order Tensor Renormalization Group. V oboch algoritmoch je základný stav multistavového spinového systému konštruovaný v tvare tenzorového súčinového stavu. Cieľom tejto práce je zovšeobecniť tieto dva algoritmy tak, aby bolo nimi možné počítať termodynamické vlastnosti neeuklidovských geometrií. Osobitne budú analyzované tenzorové súčinové stavy na hyperbolických geometriách so zápornou Gaussovou krivosťou, ale aj na fraktálnych systémoch. Následne budú vykonané rozsiahle numerické simulácie multistavových spinových modelov. Tieto spinové systémy boli zvolené pre ich vhodnosť správne modelovať základné vlastnosti zložitejších systémov, akými sú sociálne správanie, neurónové siete, holografický princíp, vrátane teórie korešpondecie medzi anti-de Sitterovým priestorom a konformnou teóriou poľa v kvantovej gravitácii. Táto práca obsahuje nové postupy aplikácie tenzorových sietí a umožňuje pochopiť fázové prechody a kvantovú previazanosť interagujúcich systémov na neeuklidovských geometriách. Budeme sa preto bližšie venovať nasledujúcim trom tematickým oblastiam. (1) Navrhneme nový termodynamický model sociálneho vplyvu, v ktorom budeme vyšetrovať fázové prechody. (2) Na nekonečnej množine geometrií so zápornou krivosťou klasifikujeme a analyzujeme fázové prechody pomocou voľnej energie. Zároveň bude stanovený vzťah, ktorý dáva do súvisu voľnú energiu a Gaussov polomer krivosti. (3) Navrhneme nový algoritmus založený na tenzorových sieťach, ktorý umožní študovať fázové prechody na nekonečne veľkých fraktálnych štruktúrach.

Kľúčové slová:
Klasifikácia fázových prechodov, Kvantové a klasické spinové mriežkové modely, Tenzorové súčinové stavy, Tenzorové siete, Renormalizácia matice hustoty

Abstract

One of the challenging problems in the condensed matter physics is to understand the quantum many-body systems, especially, physical mechanisms behind. Since there are only a few complete analytical solutions of these systems, several numerical simulation methods have been proposed in recent years. Amongst all of them, the *Tensor Network* algorithms have become increasingly popular in recent years, especially for their adaptability to simulate strongly correlated systems. The current work focuses on the generalization of such Tensor-Network-based algorithms, which are sufficiently robust to describe critical phenomena and phase transitions of multistate spin Hamiltonians in the thermodynamic limit. Therefore, one has to deal with systems of infinitely many interacting spin particles. For this purpose, we have chosen two algorithms: the Corner Transfer Matrix Renormalization Group and the Higher-Order Tensor Renormalization Group. The ground state of those multistate spin systems in the thermodynamic equilibrium is constructed in terms of a tensor product state ansatz in both of the algorithms. The main aim of this work is to generalize the idea behind these two algorithms in order to be able to calculate the thermodynamic properties of non-Euclidean geometries. In particular, the tensor product state algorithms of hyperbolic geometries with negative Gaussian curvatures as well as fractal geometries will be theoretically analyzed followed by extensive numerical simulations of the multistate spin models. These spin systems were chosen for their applicability to mimic the intrinsic properties of much more complex systems of social behavior, neural network, the holographic principle, including the correspondence between the anti-de Sitter and conformal field theory in quantum gravity. This work contains novel approaches in tensor networks and opens the door for the understanding of phase transition and entanglement of the interacting systems on the non-Euclidean geometries. The following three topics are investigated by means of the tensor-based algorithms. (1) A new thermodynamic model of social influence is proposed, and its phase transition phenomena are studied. (2) The phase transitions are classified and analyzed by the free energy on an infinite set of the negatively curved geometries. A relation between the free energy and the Gaussian radius of the curvature is conjectured. (3) A unique tensor-based algorithm is proposed, which enables to treat the phase transition on infinitely large fractal structures.

Keywords:
Phase Transition Phenomena, Quantum and Classical Spin Lattice Models,
Tensor Product States, Tensor Networks, Density Matrix Renormalization

1. Introduction

The mathematical treatment of the collective behavior of many-body systems is a highly nontrivial task. Even knowing the underlying laws of microscopic interactions does not guarantee that one can say anything specific about the large-scale behavior of the studied system. The application of the laws might lead to equations which are too complex to be solved. Even worse, the difficulty is usually nested one level deeper, and the Hilbert space is far too large to be treated thoroughly. For instance, if considering a system of N interacting particles with the spin one-half on a discrete lattice, the full description of the ground state only requires to know 2^N complex amplitudes. For more realistic systems (like a tiny piece of a magnet), the number of particles is $N \gtrsim 10^{23}$, which makes number of the basis states larger than the number of all particles in the observable Universe.

Fortunately, not all states are created equally. Nature seems to prefer systems with local interactions only (loosely speaking, the nearest and/or the second nearest particles dominantly contribute to the mutual interactions). Consequently, the Hilbert space of such interaction-restricted systems gets significantly reduced. The low-energy states of such systems (with gapped Hamiltonians) constitute only a tiny corner of all the possible states. Those states satisfy the so-called *area law* for the entanglement entropy S, which scales with the surface of a subsystem A, i.e., $S \sim \partial A$ (note that the entropy is not proportional to the volume of A).

Therefore, having developed an appropriate tool to solve such systems, which efficiently represents that tiny corner of the area-law, is to be of a great advantage. This is certainly the main reason why there is an increasing interest in formulations of suitable numerical algorithms to cope with all those non-trival tasks of quantum physic. Recently, the *tensor networks* proved to be the right mathematical concept, which is powerful enough to yield the correct answers.

The present PhD thesis deals with the phase transition phenomena, where the area law is not applicable. For this reason, the difficulty of performing the task dramatically increases. Nevertheless, the tensor network formalism is capable of representing the entanglement of the systems efficiently and correctly, noticing that the higher the interaction structure of the underlaying lattice geometry, the more complex tensor networks have to be constructed. The tensor networks formalism in connection with the renormalization group is a right choice to carry out the numerical calculations with in the thermodynamic limit, $N \to \infty$.

Therefore, the underlying topology of the interactions in the system plays a crucial role in determining the thermodynamic properties of an interacting model. For simplicity, we focus on multistate spin models, which are the typical candidates for the magnetic systems exhibiting first- and the second-order phase transitions. Specifically, we are greatly interested in study of the phase transition phenomena on non-Euclidean lattices, in particular, on hyperbolic surface geome-

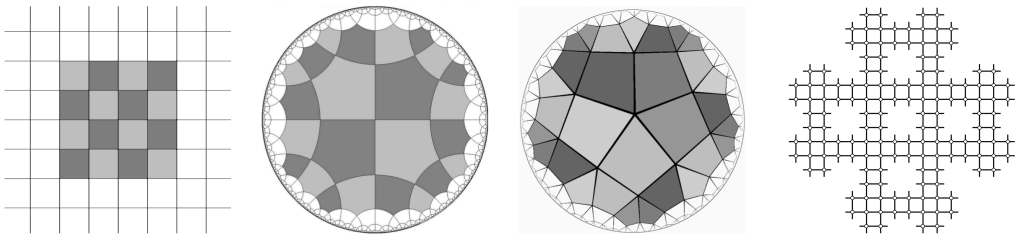

Figure 1: The illustration of four typical lattice geometries: (from left to right) the Euclidean square lattice, the two hyperbolic lattices, and the fractal lattice.

tries, which have an infinite effective spatial dimension ($d \to \infty$) with a constant negative curvature as well as on fractal geometries with the fractional dimensions $1 < d < 2$. The four typical examples of the lattice geometry of finite size are depicted in Fig. 1, i.e., the Euclidean square lattice (left), two hyperbolic lattices in Poincaré disk representation (in the middle) and the fractal lattice (right).

One of the main purposes for researching the phase transition phenomena of spin systems on the non-Euclidean lattice geometries is the fact that these systems have been found to be neither exactly solvable nor numerically feasible by standard methods such as Monte Carlo simulations, exact diagonalization, Density Matrix Renormalization Group, Projected Entangled Pair States, etc. We, therefore, proposed generalized numerical algorithms based on the Tensor Network ideas, to be able to solve the thermodynamic properties of various spin systems on the hyperbolic and the fractal lattices of infinite sizes. The algorithms reach a sufficiently high numerical accuracy being sufficient for classifying the phase transitions including the evaluation of the associated critical exponents. We have successfully achieved novel results, which have been missing in the theory of solid state physics, statistical mechanics, quantum information theory, as well as in the anti-de Sitter space of the general theory of relativity. The results of our studies have been published in Refs. [10, 11, 17].

The results are briefly summarized into three sections following the most significant results of the respective published papers. Section 3 shows the main results of a multistate spin model, which we have proposed in order to mimic social behavior of communicating individuals. The proposed thermodynamic model has been inspired by Axelrod model [1]. Section 2 contains the novel numerical results of our study based on our analytic derivation of the free energy for an infinite set of hyperbolic lattice geometries via recurrence relations. The phase transition on the fractal geometries is analyzed in Section 4. We proposed a fractal lattice, where the simple Ising model can act. The properties of the fractal lattice enabled us to construct such a tensor network, which is algorithmically tractable by means of a modified method called Higher-Order Tensor Renormalization Group.

2. Thermodynamic model of social influence

A classical spin lattice model is considered on the regular two-dimensional square lattice, where the nearest-neighbor multistate spins can interact. Let $\sigma_{i,j} = 0, 1, \ldots, q-1$ be a generalized multi-spin with integer degrees of freedom n. The subscript indices i and j denote the position of each lattice vertex, where the spins are placed within the X and Y coordinate system on the underlying lattice, i.e., $-\infty < i, j < \infty$. The interaction term, J, acts between the nearest-neighbor vector spins $\theta_{i,j} = 2\pi\sigma_{i,j}/n$. Such a system is known as the q-state clock model. The further generalization of the clock model gives the interaction term J a special attribute, i.e., extra spins are added. Therefore, additional degrees of freedom to each vertex are introduced. The position dependent term J_{ijk} describes the spin interactions J of the n-state clock model being controlled by an additional q-state Potts model δ-interactions [21]. The total number of the spin degrees of the freedom is nq on each vertex i, j.

Finally, our multi-state spin model contains two q-state spins on the same vertex, i.e., $\sigma^{(1)}_{i,j} = 0, 1, 2, \ldots, q-1$ and $\sigma^{(2)}_{i,j} = 0, 1, 2, \ldots, q-1$, which are distinguished by the superscripts (1) and (2). It is instructive to introduce a q^2-variable $\xi_{i,j} = q\sigma^{(1)}_{i,j} + \sigma^{(2)}_{i,j} = 0, 1, \ldots, q^2-1$. The Hamiltonian of our thermodynamic model has the final form

$$\mathcal{H} = \sum_{i,j=-\infty}^{\infty} \sum_{k=0}^{1} \left\{ J^{(1)}_{ijk} \cos\left[\theta^{(2)}_{i,j} - \theta^{(2)}_{i+k,j-k+1}\right] + J^{(2)}_{ijk} \cos\left[\theta^{(1)}_{i,j} - \theta^{(1)}_{i+k,j-k+1}\right] \right\},$$

noticing that $\theta^{(\alpha)}_{i,j} = 2\pi\sigma^{(\alpha)}_{i,j}/q$, where

$$J^{(\alpha)}_{ijk} = -J\delta\left(\sigma^{(\alpha)}_{i,j}, \sigma^{(\alpha)}_{i+k,j-k+1}\right) \equiv \begin{cases} -J, & \text{if } \sigma^{(\alpha)}_{i,j} = \sigma^{(\alpha)}_{i+k,j-k+1}, \\ 0, & \text{otherwise.} \end{cases}$$

The superscript (α) can take only two values as described above. The k summation includes the horizontal and the vertical directions on the square lattice. The Potts-like interaction $J^{(\alpha)}_{ijk}$ is represented by a diagonal $q \times q$ matrix with the elements $-J$ on the diagonal.

Thus defined model describes conditionally communicating (interacting) individuals of a society. The society is modeled by individuals ($\xi_{i,j}$) and each individual has two distinguished features $\sigma^{(1)}$ and $\sigma^{(2)}$. Each feature assumes q different values (traits). In particular, an individual positioned on $\{i, j\}$ vertex of the square lattice communicates with a nearest neighbor, say $\{i+1, j\}$, by comparing the spin values of the first feature $\sigma^{(1)}$. This comparison is carried out by means of the q-state Potts interaction. If the Potts interaction is non-zero, the individuals communicate via the q-state clock interaction of the other feature with $\alpha = 2$. The

cosine enables a broader communication spectrum than the Potts term. Since we require symmetry in the *Potts-clock* conditional communication, we include the other term in the Hamiltonian, which exchanges the role of the features (1) and (2) in our model. In particular, the Potts-like communication first compares the feature $J^{(2)}_{ijk}$ followed by the cosine term with the feature $\alpha = 1$. (Enabling extra interactions between the two features within each individual and/or the cross-interactions of the two adjacent individuals is to be studied elsewhere.) The total number of all the individuals is considered to be infinite in order to detect and analyze the phase transition when the spontaneous symmetry breaking is present.

In the framework of the statistical mechanics, we investigate a combined q-state Potts and q-state clock model which is abbreviated as the q^2-state spin model. As an example, one can interpret the case of $q = 3$ in the following: the feature $\sigma^{(1)}$ can be chosen to represent *leisure-time interests* while the other feature $\sigma^{(2)}$ can involve *working duties*. In the former case, one could list three properties such as reading books, listening to music, and hiking, whereas the latter feature could consist of manual activities, intellectual activities, and creative activities, as the example. The thermal fluctuations, induced by the thermodynamic temperature T of the Gibbs distribution, are meant to describe a *noise* hindering the communication. The higher the noise, the stronger suppression of the communication is results.

In order to classify the phase transitions of our model, we calculate the partition function $\mathcal{Z} = \mathrm{Tr}\, \exp(-\mathcal{H}/T)$ numerically. The communicating noise is associated with the thermodynamic temperature T. The partition function is evaluated numerically by the CTMRG algorithm [15], which generalizes the Density Matrix Renormalization Group [20] on the two-dimensional classical spin systems.

Figure 2 shows the case of $q = 2$ resulting in the four different scenarios of the order parameter $\langle O \rangle = \mathrm{Tr}_s\{\cos[2\pi(\xi - \phi)/q^2]\hat{\rho}_s\}$ (here, $\hat{\rho}_s$ being the reduced density matrix). These scenarios are depicted by the black circles ($\phi = 0$), the red diamonds ($\phi = 1$), the blue squares ($\phi = 2$), and the green triangles ($\phi = 3$). They correspond to the following vertex configurations $|\uparrow\uparrow\rangle$, $|\uparrow\downarrow\rangle$, $|\downarrow\uparrow\rangle$, and $|\downarrow\downarrow\rangle$, respectively.

At zero temperature there are three minima of the free energy leading to the three different complete order parameters $\langle O \rangle$ being -1, 0, and $+1$. There are four minima of the free energy if $0 < T < T_{c,1}(q = 2)$ so that the order parameter has four different values $\langle O \rangle = -1 + \varepsilon$, $-\varepsilon$, $+\varepsilon$, and $+1 - \varepsilon$ with the condition $0 < \varepsilon \leq \frac{1}{2}$. It means the two states share the same free energy minimum when the order parameter is zero at $T = 0$ and $\varepsilon = 0$. In the temperature interval $T_{c,1}(2) \leq T < T_{c,2}(q = 2)$, there are only two free energy minima present and the order parameter pair for $\phi = 0$ and $\phi = 3$ becomes identical as well as the pair for $\phi = 1$ and $\phi = 2$. The only single free energy minimum is resulted at $T \geq T_{c,2}(q = 2)$ when the order parameter is zero, which is typical for the disordered phase. The

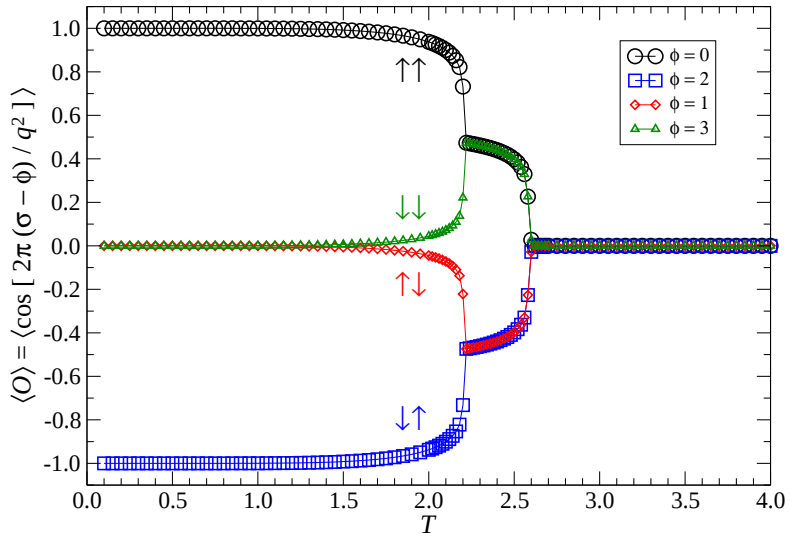

Figure 2: The complete order parameter acting on the q^2-state variable ξ exhibits the presence of the two phase transition temperatures if $q = 2$ and $f = 2$. All of the four reference spin levels (labeled by ϕ) are displayed after the spontaneous symmetry breaking occurs.

two temperatures, $T_{c,1}(q = 2)$ and $T_{c,2}(q = 2)$, correspond to two distinct phase transitions of the model,

Let us stress that at the temperatures in between $T_{c,1}(2)$ and $T_{c,2}(2)$, the pair of the site configurations $|\uparrow\uparrow\rangle$ and $|\downarrow\downarrow\rangle$ is indistinguishable by the complete order parameter (i.e. the black and green symbols coincide), and the same topological uniformity happens for the pair of the site configurations $|\uparrow\downarrow\rangle$ and $|\downarrow\uparrow\rangle$.

Extrapolating the number of the spin degrees of freedom $q \to \infty$, a non-zero phase transition point $T_t(\infty)$ is resulted. The three independent extrapolations are depicted in Fig. 3. All of them resulted in the transition point $T_t(\infty) \approx 0.5$. We, therefore, conjectured the existence of the ordered phase below the non-zero phase transition point $T_t(q)$, which persists for any $q \geq 2$.

Our thermodynamic model of the social system exhibits two phase transitions when $q = 2$. Using the above-mentioned examples, one can interpret results in the following: let, for instance, the first feature describe the two activities: 'reading of books' ($\sigma^{(1)} = \uparrow$) and 'listening to music' ($\sigma^{(1)} = \downarrow$), whereas the second two-state feature involves 'manual activity' ($\sigma^{(2)} = \uparrow$) and 'intellectual activity' ($\sigma^{(2)} = \downarrow$). Both of the phase transitions are continuous separating three phases, which are classified into (i) the low-noise regime, (ii) the medium-noise regime, and (iii) the high-noise regime.

(i) In the low-noise regime, the individuals tend to form a single dominant cluster, where the complete order parameter has four values (three if $T = 0$ only),

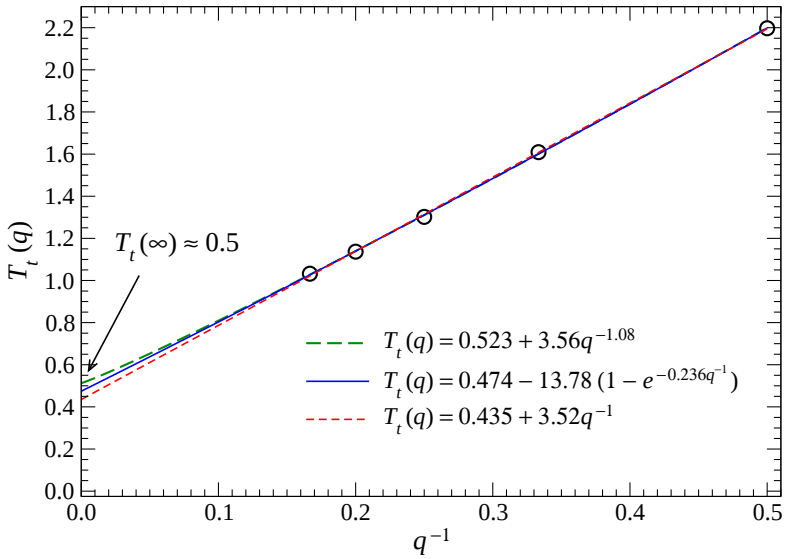

Figure 3: The there variants of the extrapolated transition temperature $T_t(q \to \infty)$ by the power-law fitting (the green long-dashed line), the exponential fitting (the blue full line), and the inverse proportionality (the red short-dashed line).

see Fig. 2. The statistical probability of forming the dominant clusters is proportional to $\langle O \rangle$. If the noise increases and the complete order parameter decreases to the values of $\langle O \rangle = \frac{1}{2}$, the four different clusters are formed, and a final size of the dominant cluster (chosen be setting the parameter ϕ) decreases proportionally to this complete order parameter. (ii) In the medium-noise regime, an interesting topological regime reveals just two equally likely traits of the individuals. In the social terms, the pairing of the cultural settings coincides either with (1) the equal mixture of those individuals who 'read books' and 'do manual activity' ($\uparrow\uparrow$) and the individuals who 'listen to music' and 'do intellectual activity' ($\downarrow\downarrow$) or (2) the equal mixture of those who 'listen to music' and 'do manual activity' ($\downarrow\uparrow$) and those who 'read books' and 'do intellectual activity' ($\uparrow\downarrow$). (iii) In the high-noise regime, the clusters are not significant (the correlation length decreases to zero if the noise increases), and the individuals behave in a completely uncorrelated way. By tuning the noise (temperature T), the formation of the clusters of various sizes is possible. The inclusion of an external magnetic field (representing mass media or advertisement) in a specific direction, the social behavior can be controlled. The only one phase transition of the first order is present for the number of the traits $q > 2$, and much richer scale of social behavior is possible being well-controlled by the external parameter (e.g., by the mass media).

3. Free energy on hyperbolic geometries

The idea of replacing the standard transfer matrix formulation of classical spin systems by the alternative corner transfer matrix method originates in Baxter's proposal of treating spin Hamiltonians [2]. The reformulation of Baxter's analytical study into the numerical CTMRG algorithm was first performed by Nishino and Okunishi [15, 16], who combined the corner transfer matrix formalism with the numerically effective Density Matrix Renormalization Group method [20]. In 2007, the CTMRG algorithm was generalized and applied to the Ising model on the pentagonal hyperbolic lattice with the constant coordination number four [18].

The essence of the CTMRG algorithm lies in finding the recurrence relations, which are used for the extension of the corner transfer matrices. Before we propose a unified CTMRG algorithm for any classical spin system on the hyperbolic lattice surfaces, we describe the lattice geometry that is gradually built up by polygons. Let the lattice be made by the regular polygonal tessellation with the constant coordination number. Each lattice geometry is characterized by the Schläfli symbol (p,q), where p is associated with the regular polygon of p sides (the p-gon in the following) with the constant coordination number q.

There are three possible scenarios of creating the lattice geometry (p,q) for the integers $p > 2$ and $q > 2$. (1) The condition $(p-2)(q-2) = 4$ gives rise to the two-dimensional Euclidean flat geometry. In this study, we consider only the square lattice $(4,4)$, which satisfies the condition, and the remaining triangular $(3,6)$ and honeycomb $(6,3)$ Euclidean lattices will be studied elsewhere. (2) If $(p-2)(q-2) > 4$, the infinite set of the hyperbolic geometries can satisfy the condition. Although such lattices of infinite size define various two-dimensional curved surfaces, the entire infinite hyperbolic lattice can be spanned in the infinite-dimensional space only; it is commonly associated with the Hausdorff dimension which is infinite. None of the hyperbolic lattices can be endowed in the three-dimensional space. (3) The condition $(p-2)(q-2) < 4$ corresponds to only five finite-sized spherically curved geometries, which are trivial and are not considered in the current study.

Each vertex of the infinite (p,q) lattice, built up by the p-gons with the fixed coordination number q, represents a classical multi-spin variable σ interacting with the q nearest-neighboring spins. The Hamiltonian $\mathcal{H}_{(p,q)}$ can be decomposed into the sum of identical local Hamiltonians $\mathcal{H}_p$ acting exclusively on the local p-gons, which are considered to be the basic elements in the construction of the entire lattice. In particular, the decomposition of the full Hamiltonian is

$$\mathcal{H}_{(p,q)}\{\sigma\} = \sum_{(p,q)} \mathcal{H}_p[\sigma],$$

where the sum is taken through the given lattice geometry (p,q) accordingly. The

simplified spin notations $[\sigma]$ and $\{\sigma\}$, respectively, are ascribed to the p spins within each local Hamiltonian $\mathcal{H}_p[\sigma] \equiv \mathcal{H}_p(\sigma_1\sigma_2\cdots\sigma_p)$ and the infinitely many spins $\{\sigma\}$ of the entire system $\mathcal{H}_{(p,q)}\{\sigma\} \equiv \mathcal{H}_{(p,q)}(\sigma_1\sigma_2\cdots\sigma_\infty)$. We consider two types of the multi-state spin models: the M-state clock model with the local Hamiltonian

$$\mathcal{H}_p[\sigma] = -J\sum_{i=1}^{p}\cos\left[\frac{2\pi}{M}(\sigma_i - \sigma_{i+1})\right]$$

and the M-state Potts model

$$\mathcal{H}_p[\sigma] = -J\sum_{i=1}^{p}\delta_{\sigma_i,\sigma_{i+1}},$$

where $\sigma_{p+1} \equiv \sigma_1$ within the p-gon, and where each M-state spin variables $\sigma = 0, 1, 2, \ldots, M-1$. (Thus, the Ising model is associated with $M = 2$.) We consider the ferromagnetic interaction $J > 0$ to avoid frustration.

Let the Boltzmann weight $\mathcal{W}_\mathrm{B}[\sigma] = \exp(-\mathcal{H}_p[\sigma]/k_\mathrm{B}T)$ be defined on the p-gon of the local Hamiltonian, where k_B and T correspond to the Boltzmann constant and temperature, respectively. We use the dimensionless units throughout this work and set $J = k_\mathrm{B} = 1$. In general, the Ising model on the hyperbolic lattices (p,q) is not exactly solvable, except for special asymptotic cases, on the Bethe lattices, as discussed later. We employ the CTMRG algorithm as a powerful tool to study the phase transitions numerically on the arbitrary lattice geometries (p,q). We check the correctness and accuracy of the results by comparing the phase transition temperatures with the exactly solvable Ising model on the Bethe lattices [2].

The iterative expansion process is formulated in terms of the generalized corner transfer matrix notation (for details, see Refs. [8, 9, 12, 18]), where the corner transfer tensors C_j and the transfer tensors $\mathcal{T}_j$ expand their sizes as the iteration step (indexed by j) increases, i.e. $j = 1, 2, 3, \ldots, k$. Having analyzed all the geometrical lattice structures (p,q) of the polygonal tailing, it straightforwardly leads to the recurrence relations

$$\begin{aligned} C_{j+1} &= \mathcal{W}_\mathrm{B}\mathcal{T}_j^{p-2}C_j^{(p-2)(q-3)-1}, \\ \mathcal{T}_{j+1} &= \mathcal{W}_\mathrm{B}\mathcal{T}_j^{p-3}C_j^{(p-3)(q-3)-1}. \end{aligned}$$

The partition function, $\mathcal{Z}_{(p,q)}^{[k]}$, in the final k^th iteration step is given by the configuration sum (or, equivalently, by the trace) of the product of the q corner transfer tensors, which are concentrically connected around the central spin site of the lattice [18]

$$\mathcal{Z}_{(p,q)}^{[k]} = \mathrm{Tr}\left[e^{-\mathcal{H}_{(p,q)}/T}\right] = \mathrm{Tr}\,(\underbrace{C_kC_k\cdots C_k}_{q}) \equiv \mathrm{Tr}\,(C_k)^q.$$

Let the free energy for any lattice geometry (p,q) be normalized per lattice spin site to avoid any divergences associated with the thermodynamic limit. The free energy per site, expressed as a function of the iteration step k, has the form

$$\mathcal{F}^{[k]}_{(p,q)} = -\frac{T}{\mathcal{N}^{[k]}_{(p,q)}} \ln \mathcal{Z}^{[k]}_{(p,q)} \equiv -\frac{T \ln \mathrm{Tr}\,(C_k)^q}{\mathcal{N}^{[k]}_{(p,q)}},$$

The generalization of the free energy calculation for any (multi-state) spin model on an arbitrary lattice geometry $(p \geq 4, q \geq 4)$ is straightforward and requires a careful graphical analysis of many lattice geometries, which is beyond the scope of this work for its extensiveness. The free energy per spin for a finite k has the generalized form

$$\mathcal{F}^{[k]}_{(p,q)} \overset{k \gg 1}{=} -\frac{qT \sum\limits_{j=0}^{k-1} n_{j+1} \ln c_{k-j} + m_{j+1} \ln t_{k-j}}{1 + q \sum\limits_{j=1}^{k} (p-2) n_j + (p-3) m_j}.$$

The integer functions n_j and m_j satisfy more complex recurrence relations

$$\begin{aligned} n_{j+1} &= [(p-2)(q-3)-1] n_j + [(p-3)(q-3)-1] m_j, \\ m_{j+1} &= (p-2) n_j + (p-3) m_j. \end{aligned}$$

being initialized by $n_1 = 1$ and $m_1 = 0$.

Having been motivated by the correspondence between the anti-de Sitter spaces and the conformal field theory of the quantum gravity physics, one can put the question: *"Given an arbitrary spin system on an infinite set of (p,q) geometries, which lattice geometry minimizes the free (ground-state) energy?"*. This is certainly a highly non-trivial task to be explained thoroughly. Nevertheless, we attempt to answer the question in the following for a particular set of curved lattice surfaces we have been considering. This helps us give an insight into the role of the space geometry with respect to the microscopic description of the spin interacting system. Although we currently consider the free energy of the *classical* spin lattice systems, we have been recently studying the ground-state energy of the *quantum* spin systems on the lattices $(p \geq 4, 4)$, which also exhibit qualitatively identical features as studied in this work [5, 6]. For this reason, the free energy for classical spin systems and the ground-state energy of quantum spin systems are mutually related.

The free energy per site $\mathcal{F}^{[\infty]}_{(p,q)}$ converges to a negative value $\mathcal{F}^{[\infty]}_{(p,q)} < 0$ at finite temperatures $T < \infty$ in the thermodynamic limit. Scanning the entire set of the $(p \geq 4, q \geq 4)$ geometries, we show in the following that the free energy per site

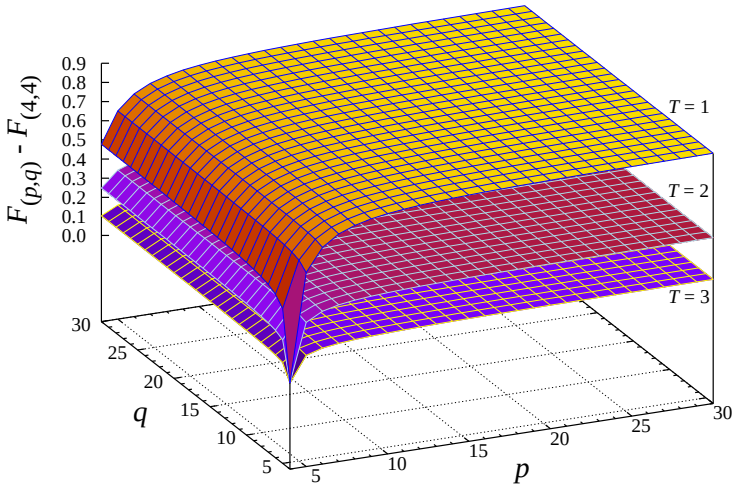

Figure 4: The free energy per site as a function of the lattice geometry (p,q) at the selected lower temperatures $T = 1, 2$, and 3.

reaches its minimum on the square lattice only

$$\mathcal{F}^{[\infty]}_{(4,4)} = \min_{(p\geq 4, q\geq 4)} \left\{ \mathcal{F}^{[\infty]}_{(p,q)} \right\}$$

at any fixed temperature T. For clarity of the figures, we plot the *shifted* free energy per site, $\mathcal{F}^{[\infty]}_{(p,q)} - \mathcal{F}^{[\infty]}_{(4,4)} \geq 0$.

Figure 4 shows the shifted free energy for the Ising ($M = 2$) model. These numerical calculations unambiguously identify the square lattice geometry, which minimizes the free energy per spin site. It is worth to mention that the existence of the phase transition does not affect the free energy minimum observed on the Euclidean square lattice. Moreover, as the temperature grows, the difference between the free energies on the square and the hyperbolic lattices weakens.

The studied (p,q) lattices can be exactly characterized by the radius of Gaussian curvature [14], which has the analytical expression

$$\mathcal{R}_{(p,q)} = -\frac{1}{2\,\mathrm{arccosh}\left[\frac{\cos\left(\frac{\pi}{p}\right)}{\sin\left(\frac{\pi}{q}\right)}\right]}.$$

For later convenience, we include the negative sign in $\mathcal{R}_{(p,q)}$. The radius of curvature for the square lattice geometry $(4,4)$ diverges, $R_{(4,4)} \to -\infty$, while the remaining hyperbolic lattice geometries (p,q) are finite and non-positive. The analytical expression for $\mathcal{R}_{(p,q)}$ results in a constant and position independent curvature at

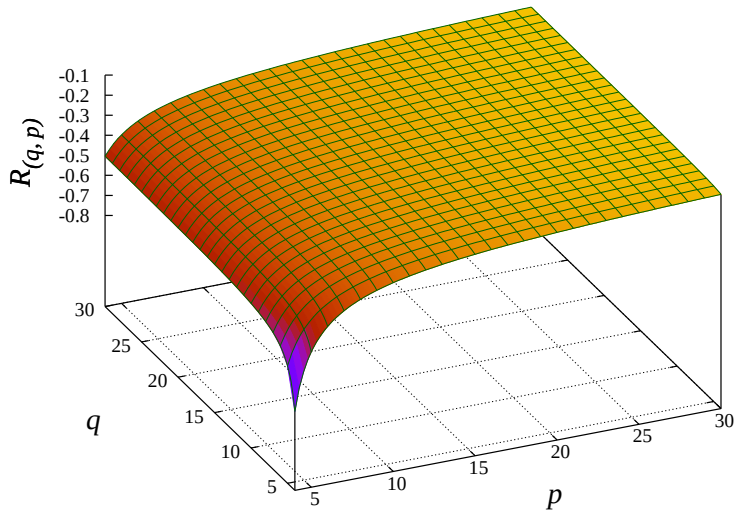

Figure 5: The functional dependence of the Gaussian radius of curvature $\mathcal{R}_{(q,p)}$ plotted in the dual lattice geometry (q,p).

any position on the infinitely large lattices (p,q). It is a consequence of the constant distance between the lattice vertices for all geometries (p,q), which is equivalent to keeping the spin-spin coupling to be $J=1$ in all the numerical analysis of the spin systems on the (p,q) lattices.

In Fig. 5 we plot the radius of curvature in the dual geometry (q,p), i.e., the roles of p and q are swapped. It is immediately evident that the surface shape of $\mathcal{R}_{(q,p)}$ exhibits a qualitative similarity if compared to the free energy per site $\mathcal{F}^{[\infty]}_{(p,q)}$ we depicted in Fig. 4. Such a surprising observation opens new questions about the relation between the energy at thermal equilibrium and the space (lattice) geometry, which is equivalent to the relation between the ground-state energy of quantum systems and the underlying geometry.

It is instructive to inspect the asymptotic behavior of $\mathcal{R}_{(q,p)}$. If q is fixed to an arbitrary $q^* \geq 4$, the logarithmic dependence on p is present and $\mathcal{R}_{(q^*,p\gg 4)} \rightarrow -1/2\ln[\frac{2p}{\pi}\cos(\frac{\pi}{q^*})]$. Fixing p to p^* causes that the radius of curvature converges to a constant so that for a sufficiently large p^*, the constant does not depend on q and $\mathcal{R}_{(q\gg 4,p^*)} \rightarrow -1/2\ln[\frac{2}{\sin(\pi/p^*)} - \frac{\sin(\pi/p^*)}{2}] \approx -1/\ln(\frac{2p^*}{\pi})^2$. It is straightforward to conclude that the asymptotics of $\mathcal{R}_{(q,p)}$ is solely governed by the parameter p, i.e. $\mathcal{R}_{(q\gg 4,p\gg 4)} \rightarrow -1/2\ln(\frac{2p}{\pi})$.

We conjecture the following asymptotic relation between the free energy per site and the radius of curvature on the dual lattice geometry

$$\mathcal{F}^{[\infty]}_{(p,q)} - \mathcal{F}^{[\infty]}_{(\infty,q)} \propto \frac{\partial}{\partial p}\mathcal{R}^{-1}_{(q,p)} \approx -\frac{\pi}{2}\exp\left[\frac{1}{2}\mathcal{R}^{-1}_{(q,p)}\right],$$

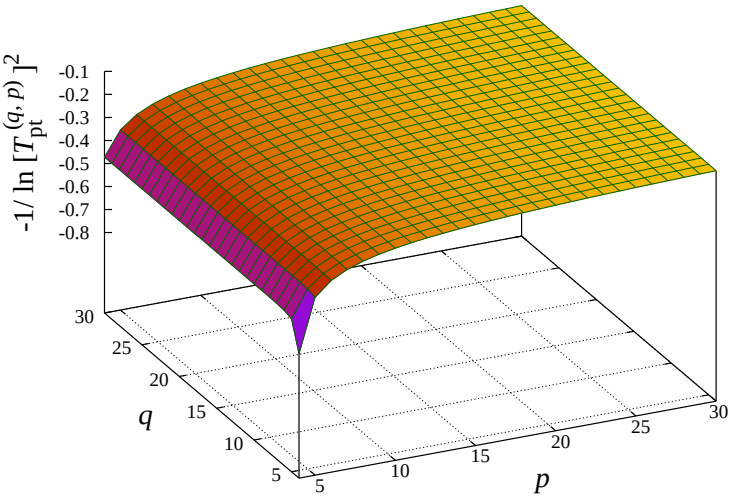

Figure 6: The rescaled phase transition temperatures with respect to p and q are shown in the dual geometry (q,p) to emphasize the similarity with the radius of Gaussian curvature in Fig. 5.

which is valid for any fixed $q \geq 4$ and $p \gg 4$ (typically $p \gtrsim 10^2$) at low temperatures. Necessity to perform other studies is inevitable to support our findings. The consequences of the current work are expected to elicit further research, which can bridge the quantum physics with the general theory of relativity.

Having analyzed the phase transition temperatures $T_{\rm pt}^{(p,q)}$ of the Ising model with respect to the lattice geometries (p,q), we again find another analogous relation for the scaling of the radius of Gaussian curvature

$$-1/\ln\left[T_{\rm pt}^{(p,q)}\right]^2 \propto \mathcal{R}_{(p,q)}$$

as shown in Fig. 6. For the better visual comparison with Fig. 5, we plotted $-1/[2\ln T_{\rm pt}^{(p,q)}]$ in the dual geometry (i.e., the meanings of p and q are swapped in the graph). Recall that the higher values of the coordination number q (for fixed p) cause that $T_{\rm pt}^{(p,q)} \propto q$, whereas if p increases (at fixed q), the fast convergence to $2/\ln[q/(q-2)]$ is achieved.

Hence, the evident mutual similarity of the functional p,q-dependence among the free energy per site in Fig. 4, the radius of the Gaussian curvature in Fig. 5, and the phase transition temperature in Fig. 6 leads us to conjecture that a theoretical explanation should exist, which connects them all together. Or, in other words, our findings call for the necessity to formulate an appropriate theoretical background.

4. Fractal geomeries

Compared with critical phenomena on regular lattices, much less is known on fractal lattices. For example, the Ising model on the Sierpinski gasket does not exhibit phase transition at any finite temperature, although the Hausdorff dimension of the lattice, $d_{\mathrm{H}} = \ln 3/\ln 2 \approx 1.585$, is larger than one [7, 13]. The absence of the phase transition could be explained by the fact that the number of interfaces, i.e. the outgoing bonds from a finite area, does not increase when the size of the area is doubled on the gasket. In case of the Ising model on the Sierpinski carpet, presence of the phase transition is proved [19], and its critical indices were roughly estimated by Monte Carlo (MC) simulations [4]. It should be noted that it is not easy to collect sufficient number of data plots for finite-size scaling [3] on such fractals by means of MC simulations due to the exponential increase of the number of sites in a unit cell of the fractal.

The classical Ising model is investigated on a planar fractal lattice, as shown in Fig. 1(right). The fractal lattice consists of the vertices around the lattice points, which are denoted by the empty dots in the figure, where the Ising spins are placed. The whole lattice is constructed by recursive extension processes, where the linear size of the system increases by the factor of four in each step. If the lattice is a regular square one, $4 \times 4 = 16$ units are connected in the extension process, whereas only 12 units are connected on this fractal lattice; the 4 units are missing in the corners. As a result, the number of sites contained in a cluster after n extensions is $N_n = 12^n$, and the Hausdorff dimension of this lattice is $d_{\mathrm{H}} = \ln 12/\ln 4 \approx 1.792$. The number of outgoing bonds from a cluster is only doubled in each extension process since the sites and the bonds at each corner are missing. If we evaluate the lattice dimension from the relation $M = L^{d-1}$ between the linear dimension L and the number of outgoing bonds M, we have $d = 1.5$. It is so because M is proportional to $\sqrt{L}$ on the fractal. Remark that the value is different from $d_{\mathrm{H}} \approx 1.792$.

We report the critical behavior of the Ising model on the fractal lattice when the system size is large enough. Thermodynamic properties of the system are numerically studied by means of the Higher-Order Tensor Renormalization Group method [22]. The spin system exhibits a single order-disorder phase transition, where the critical indices are different from the square-lattice Ising model.

Figure 7(left) shows the temperature dependence of the specific heat per site $c(T) = -T\partial_T^2 f(T)$, where $f(T)$ is the free energy per site in the thermodynamic limit, i.e., $f(T) = \lim_{n\to\infty} -12^{-n} k_B T \ln \mathcal{Z}$. (Here, n is number of the renormalization steps corresponding to the lattice expansion and k_B being the Boltzmann constant.) It is interesting to point out that there is no singularity in $c(T)$ around its maximum. However, one can find a weak non-analytic behavior at $T_{\mathrm{c}} \approx 1.317$, which is marked by the vertical dotted line in the figure; the numerical derivative of $c(T)$ with respect to temperature (plotted in the inset) exhibits a sharp peak at

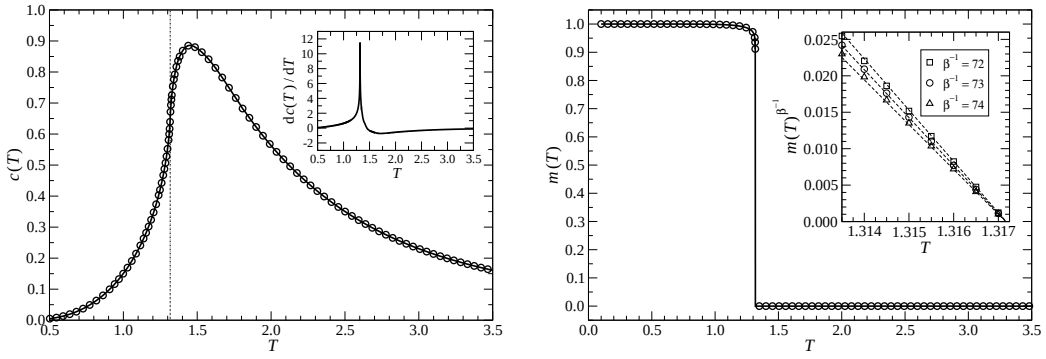

Figure 7: Left: The specific heat $c(T)$ per site. Inset: the numerical derivative of $c(T)$ with respect to temperature; a sharp peak is observed at $T_c \approx 1.317$. Right: The spontaneous magnetization per site $m(T)$. Inset: the power-law behavior below $T_c = 1.31716$.

the critical temperature T_c, which correspond to the second-order phase transition. It is numerically difficult to detect the critical exponent α (associated with the specific heat) precisely because of the weakness in the singularity.

Figure 7(right) depicts the spontaneous magnetization per site $m(T)$. Since the fractal lattice is inhomogeneous, the value is weakly dependent on the location of the observation spin site, but the critical behavior is not affected by the location. The numerical calculation captures the spontaneous magnetization $m(T)$ below T_c since any tiny round-off error is sufficient for breaking the symmetry inside low-temperature ordered state. Around the transition temperature, the magnetization satisfies a power-law behavior $m(T) \propto |T_c - T|^{1/73}$, where the precision of the exponent can be read out from the inset as a tiny deviation from the linear dependence (the dashed lines) in $m(T)^{1/\beta}$ near T_c. The calculated spontaneous magnetization $m(T)$ also supports the 2^{nd} order phase transition with the exponent $\beta_{\text{fractal}} \approx 1/73$, which is smaller by one order of magnitude than the critical exponent $\beta_{\text{square}} = 1/8$ of the square-lattice Ising model.

The lattice geometry of the fractal lattice can be modified in several manners. For example, one can alternate the system extension process of the fractal for the purpose of modifying the Hausdorff dimension; for every odd n the extension with 12 vertices shown in Fig. 1(right) is performed, and for even n the normal extension with 16 vertices on the square-lattice is performed. Alternatively, one can also modify the basic cluster, in such a manner as introducing 6 by 6 cluster where 4 corners are missing, etc. These modifications do not spoil the applicability of the numerical method used. Our further study can clarify the role of the entanglement in the universality of the phase transition.

Bibliography

[1] R. Axelrod. *The Journal of Conflict Resolution*, 42:203, 1997.

[2] R. J. Baxter. *Exactly Solved Models in Statistical Mechanics*. Academic Press, London, 1982.

[3] T. W. Burkhardt and J. M. J. van Leeuwen, editors. *Real-Space Renormalization*, volume 30 of *Topics in Current Physics*. Springer, Berlin, 1982. And references therein.

[4] J. M. Carmona, U. Marini, B. Marconi, J. J. Ruiz-Lorenzo, and A. Tarancon. *Phys. Rev. B*, 58:14387, 1998.

[5] M. Daniška and A. Gendiar. *J. Phys. A: Math. Theor.*, 48:435002, 2015.

[6] M. Daniška and A. Gendiar. *J. Phys. A: Math. Theor.*, 49:145003, 2016.

[7] Y. Gefen, A. Aharony, Y. Shapir, and B. B. Mandelbrot. *J. Phys. A*, 17:435, 1984.

[8] A. Gendiar, M. Daniška, R. Krcmar, and T. Nishino. *Phys. Rev. E*, 90:012122, 2014.

[9] A. Gendiar, R. Krcmar, S. Andergassen, M. Daniška, and T. Nishino. *Phys. Rev. E*, 86:021105, 2012.

[10] J. Genzor, V. Bužek, and A. Gendiar. *Physica A*, 420:200, 2015.

[11] J. Genzor, A. Gendiar, and T. Nishino. *Phys. Rev. E*, 93:012141, 2016.

[12] R. Krcmar, A. Gendiar, K. Ueda, and T. Nishino. *J. Phys. A*, 41:125001, 2008.

[13] J. H. Luscombe and R. C. Desai. *Phys. Rev. B*, 32:1614, 1985.

[14] R. Mosseri and J. F. Sadoc. *J. Physique - Lettres*, 43:L249, 1982.

[15] T. Nishino and K. Okunishi. *J. Phys. Soc. Jpn.*, 65:891, 1996.

[16] T. Nishino and K. Okunishi. *J. Phys. Soc. Jpn.*, 66:3040, 1997.

[17] M. Serina, J. Genzor, Y. Lee, and A. Gendiar. *Phys. Rev. E*, 93:042123, 2016.

[18] K. Ueda, R. Krcmar, A. Gendiar, and T. Nishino. *J. Phys. Soc. Jpn*, 76:084004, 2007.

[19] A. Vezzani. *J. Phys. A: Mathe. Gen.*, 36:1593, 2003.

[20] S. R. White. *Phys. Rev. Lett.*, 69:2863, 1992.

[21] F. W. Wu. *Rev. Mod. Phys.*, 54:235, 1982.

[22] Z. Y. Xie, J. Chen, M. P. Qin, J. W. Zhu, L. P. Yang, and T. Xiang. *Phys. Rev. B*, 86:045139, 2012.

Author's Publications

1. J. Genzor, V. Bužek, A. Gendiar, *Thermodynamic model of social influence on two-dimensional square lattice: Case for two features*, Physica A **420** (2015) 200

   Cited by: Y. Gandica, S. Chiacchiera, Phys. Rev. E **93** (2016) 032132

2. M. Serina, J. Genzor, Y. Lee, A. Gendiar, *Free-energy analysis of spin models on hyperbolic lattice geometries*, Phys. Rev. E **93** (2016) 042123

3. J. Genzor, A. Gendiar, T. Nishino, *Phase transition of the Ising model on a fractal lattice*, Phys. Rev. E **93** (2016) 012141